Molecular characterization of human stathmin expressed in *Escherichia coli*: site-directed mutagenesis of two phosphorylatable serines (Ser-25 and Ser-63)

Patrick A. CURMI,*§ Alexandre MAUCUER,* Sébastien ASSELIN,* Magalie LECOURTOIS,* Alain CHAFFOTTE,† Jean-Marie SCHMITTER‡ and André SOBEL*

*INSERM U153, 17 rue du Fer à Moulin, 75005 Paris, France, †CNRS URA 1129, Institut Pasteur, 28 rue du Docteur Roux, 75015 Paris, France, and ‡Laboratoire de Biochimie, Ecole Polytechnique, 92128 Palaiseau Cedex, France

Stathmin, a probable relay protein possibly integrating multiple intracellular regulatory signals [reviewed in Sobel (1991) Trends Biochem. Sci. **16**, 301–305], was expressed in *Escherichia coli* at levels as high as 20% of total bacterial protein. Characterization of the purified recombinant protein revealed that it had biochemical properties very similar to those of the native protein. It is a good substrate for both cyclic AMP-dependent protein kinase (PKA) and p34cdc2, on the same four sites as the native eukaryotic protein. As shown by m.s., the difference in isoelectric points from the native protein is probably due to the absence of acetylation of the protein produced in bacteria. C.d. studies indicate that stathmin probably contains about 45% of its sequence in an α-helical conformation, as also predicted for the sequence between residues 47 and 124 by computer analysis. Replacement of Ser-63 by alanine by *in vitro* mutagenesis resulted in a ten times less efficient phosphorylation of stathmin by PKA which occurred solely on Ser-16, confirming that Ser-63 is the major target of this kinase. Replacement of Ser-25, the major site phosphorylated by mitogen-activated protein kinase *in vitro* and *in vivo*, by the charged amino acid glutamic acid reproduced, in conjunction with the phosphorylation of Ser-16 by PKA, the mobility shift on SDS/polyacrylamide gels induced by the phosphorylation of Ser-25. This result strongly suggests that glutamic acid in position 25 is able to mimic the putative interactions of phosphoserine-25 with phosphoserine-16, as well as the resulting conformational changes that are probably also related to the functional regulation of stathmin.

INTRODUCTION

Proliferation, differentiation and cell function are controlled during development and adult life by numerous extracellular signals and intracellular regulatory cascades involving diverse signal-transduction pathways and phosphorylation–dephosphorylation reactions. We have previously identified stathmin [1,2], a ubiquitous 19 kDa cytosolic phosphoprotein, as a probable relay protein integrating diverse intracellular regulatory pathways. The same protein has also been designated p19 [3,4], pp17 or prosolin [5,6], p18 or Op18 [7–9], 19-K [10] and pp20-pp21-pp23 [11]. The expression and phosphorylation of stathmin is finely regulated in many different systems in relation to their biological, differentiation and activation states (reviewed in [2]). Phosphorylation of stathmin has been observed during physiological responses to receptor stimulation in systems as different as pituitary cells [1,12], lymphocytes [6,10,11,13–16], PC 12 cells [17], neurons [18,19] and muscle cells [20]. Expression of stathmin, which is highest in the brain [21–23] particularly in neurons [18,24,25], is also regulated in correlation with cell proliferation and differentiation: it reaches a peak in all tissues at the neonatal stage [23], is highly stimulated in T-lymphocytes in response to activating agents [26,27] and, during differentiation of several cell lines, a dramatic decrease in stathmin has been observed [4,20,27–30]. Finally, the importance of stathmin is supported by its high phylogenetic conservation [31,32], and the existence of a family of proteins containing a highly conserved stathmin domain [32,33].

Stathmin is present in cells as two isoforms, α and β [34], encoded by a single mRNA [35,36], displaying up to 14 phosphorylated forms (apparent molecular mass $\approx$ 19–23 kDa; pI $\approx$ 6.2–5.6) identified by two-dimensional electrophoresis [36,37]. Stathmin is a substrate *in vitro* for the cyclic AMP-dependent protein kinase (PKA), for cyclin-dependent kinases such as p34cdc2, and for the growth-factor-activated mitogen-activated protein (MAP) kinases. The sites phosphorylated by these kinases have been identified [37–39], and the same sites shown to be phosphorylated *in vivo* [37,40]. Furthermore, we have recently demonstrated that the four sites identified account for all the phosphoforms observed *in vivo* [37]. In particular, phosphorylation of stathmin on a specific combination of these sites is responsible for the low-mobility high-apparent-molecular-mass forms of stathmin ('16', molecular mass $\approx$ 21 kDa and, '17', molecular mass $\approx$ 23 kDa) [37]. This diversity of forms generated in response to the activation/inhibition of protein kinases and phosphatases involved in diverse regulatory cascades further supports the probable general regulatory function of stathmin.

We report here the production of recombinant human stathmin in a prokaryote expression system, and the biochemical and structural characterization of the recombinant protein. *In vitro* mutagenesis was used to produce forms of stathmin in which phosphorylation sites were replaced by a neutral or a charged amino acid: replacement of Ser-25 by glutamic acid mimics the probable structural changes and intramolecular interactions induced by the same serine in its phosphorylated state. Recom-

Abbreviations used: PKA, cyclic AMP-dependent protein kinase; MAP kinase, mitogen-activated protein kinase; IPTG, isopropyl β-thiogalactopyranoside.

§ To whom correspondence should be addressed at the above address. On leave of absence from INSERM U141, Hôpital Lariboisière, 75010 Paris, France.

binant stathmin and its mutated derivatives should prove to be valuable tools in the elucidation of the structural and functional regulation and properties of stathmin.

MATERIALS AND METHODS

Site-directed mutagenesis and construction of expression plasmids

Human stathmin cDNA [31] was first subcloned into the M13mp8 phage vector. The resulting construct was used to generate single-stranded DNA as the template for mutagenesis. To replace Ser-25 with glutamic acid (St_{25E}) and Ser-63 with alanine (St_{63A}), oligonucleotide-directed mutagenesis was carried out using the 'oligonucleotide-directed *in vitro* mutagenesis system version 2.1' (Amersham, Les Ulis, France) by following the manufacturer's instructions. The oligonucleotide primers (Genset) used to generate mutants were as follows (the mismatched bases are underlined): 25 Glu, 5'-TTCTTTTGACCGAGGCTCGAGAATCAGCTCAAA; 63 Ala, 5'-GACCTCAGCTTCATGCGCCTTGCGTCTTTCTTCTGC. Single-stranded DNA from a few clones was prepared and sequenced through the mutagenesis site by the dideoxynucleotide chain-termination method [41] using synthetic primers and a modified T7 DNA polymerase (Sequenase; US Biochemical Corp., Cleveland, OH, U.S.A.). After mutant selection, we confirmed by sequencing that no other nucleotides within the stathmin cDNA were changed during mutagenesis.

Wild-type and mutant stathmin cDNA fragments (82–1429) were subcloned into the expression vector pET-8c [42] down the T7 RNA polymerase promoter, yielding the respective plasmids pST, pSt_{25E} and pSt_{63A}.

Stathmin expression and purification

pSt, pSt_{25E} and pSt_{63A} were used to transform BL21(DE3), an *E. coli* strain harbouring the T7 RNA polymerase gene under the control of the *lac* UV5 promoter [42]. Bacteria were grown at 37 °C in Luria–Bertani medium containing 40 mg/l ampicillin. T7 RNA polymerase was induced by the addition of 0.4 mM isopropyl β-thiogalactopyranoside (IPTG) when the cells reached an A_{600} of 0.4–0.6.

Extraction and purification of wild-type and mutant recombinant stathmin were performed as follows: 4 h after induction by IPTG, cells were pelleted by centrifugation at 4 °C and resuspended in 10 vol. of TLAPE [20 mM Tris/HCl, pH 8, 10 μg/ml leupeptin, 25 μg/ml aprotinin, 10 μg/ml pepstatin (Sigma), 1 mM EDTA]. The cell suspension was sonicated twice for 60 s on ice, and the disrupted cells were centrifuged at 4 °C to give the S2 supernatant: 15 min at 3000 *g* followed by 1 h at 100000 *g*.

Stathmin was purified to homogeneity from S2 by a combination of anion-exchange chromatography and gel filtration: S2 was applied to a DEAE-Sepharose CL-6B column eluted with a 0–200 mM linear gradient of NaCl in 20 mM Tris/HCl, pH 8. Fractions containing stathmin were concentrated 10 times by evaporation, dialysed against 50 mM sodium phosphate buffer, pH 7.2, and submitted to gel filtration on a Superose 12 f.p.l.c. column (Pharmacia) to eliminate minor protein contaminants. Stathmin appeared as a single peak; the corresponding fractions were pooled and stored at −80 °C until use.

Amino acid analysis and determination of absorption coefficient of recombinant stathmin

A solution of 50 mM NH_4HCO_3 (70 and 140 μl containing about 2 and 4 nmol of pure recombinant stathmin respectively) was hydrolysed in 6 M HCl. Amino acids were then separated and quantified against known amounts of norleucine, the proportion of each amino acid being in agreement with the sequence of stathmin. This analysis was used to calibrate the u.v.-absorption spectrum of pure recombinant stathmin: absorbance values were obtained by scanning a solution of 0.68 μM pure stathmin (assuming a molecular mass of 17172 Da) in a buffer containing 50 mM NH_4HCO_3. The absorbance peak was at 199.5 nm, the absorbance at 280 nm being negligible in agreement with the absence of tyrosine and tryptophan and with a low number of phenylalanine and histidine residues in stathmin (three and four respectively). The calculated molar absorption coefficients are: $\epsilon_{205} = 526000\ M^{-1}\cdot cm^{-1}$, $\epsilon_{220} = 140000\ M^{-1}\cdot cm^{-1}$, $\epsilon_{230} = 44000\ M^{-1}\cdot cm^{-1}$, $\epsilon_{280} = 2200\ M^{-1}\cdot cm^{-1}$.

M.s.

A Fisons Instruments time-of-flight mass spectrometer (model Tofspec) equipped with a 337 nm laser was used for mass measurements, at a 25 kV acceleration voltage. Horse heart cytochrome *c* was used as an internal standard, and mass calibration was achieved with its singly and doubly charged pseudomolecular positive ions. Accurate mass measurements of recombinant stathmin were performed with its doubly charged pseudomolecular ion, bracketed by the ions of the internal standard. A 10 pmol/μl solution in 0.1 % trifluoroacetic acid was prepared for both stathmin and cytochrome *c*. Matrix solution (saturated solution of α-cyano-4-hydroxycinnamic acid in 40 % acetonitrile/0.1 % trifluoroacetic acid, 1.5 μl) was spotted on the stainless-steel multisample probe; 0.8 μl of stathmin solution and 0.2 μl of internal standard solution were successively added, and the mixture was allowed to dry at room temperature. From 80 to 150 shots were accumulated for each sample analysis.

C.d.

The far-u.v. c.d. spectrum, between 185 and 250 nm, was acquired with a Jobin-Yvon CD6 spectropolarimeter, using a 0.5 nm step. The integration time was 2 s and the bandwidth was 2 nm. Spectra were obtained by averaging three individual scans and subtracting the buffer contribution recorded under the same conditions. Protein concentration was 0.58 mg/ml (33.8 μM) based on the absorption coefficient determined at 220 nm (see above). Secondary-structure composition was estimated by a linear vectorial decomposition between 190 and 240 nm, by the method of Yang et al. [43], using the four components of Brahms and Brahms [44].

PAGE analysis

One-dimensional electrophoresis was performed on 13 % polyacrylamide gels [45]. Two-dimensional PAGE was performed as described by Garrels and Schubert [46] and Sobel and Tashjian [1]. Isoelectric-focusing gels contained 2 % total ampholines (Pharmacia), pH 5–8 and 3.5–10 in the proportion 4:1. The second dimension was on 13 % polyacrylamide gels. The gels were fixed, stained with silver or Coomassie Blue, dried and exposed to Kodak XAR-5 films for autoradiography when appropriate.

In vitro phosphorylation

Purified samples of wild-type or mutant stathmin (15 pmol) were incubated for 1 h at 30 °C with 25 units of the catalytic subunit of PKA (Sigma) and 5 μCi of [γ-^{32}P]ATP (5000 Ci/mmol) in 15 μl of 'phosphorylation buffer' [1 mM EGTA, 10 mM $MgCl_2$,

20 mM Tris/HCl (pH 7), 1 mM dithiothreitol, 1 μM ATP]. Phosphorylation with p34cdc2 (300 units) (kindly provided by Dr. M. Dorée and Dr. J. C. Labbé) was achieved in buffer composed of 10 mM $MgCl_2$, 10 mM Tris/HCl (pH 7.8), 80 mM KCl, 1 mM dithiothreitol and 1 μM ATP. The phosphorylation reactions were stopped and the samples prepared for two-dimensional gel electrophoresis with the addition of electrophoresis buffer.

Two-dimensional phosphopeptide map analysis

Phosphoproteins were located on dried Coomassie Blue-stained two-dimensional gels by superimposition on the corresponding autoradiograms, and excised. After Cerenkov counting, gel pieces were destained for 2 h with four changes of 40% methanol/10% acetic acid and washed for 2 h with 50% methanol. Samples were lyophilized and submitted to successive digestions by trypsin and thermolysin as described by Beretta et al. [37]. The first digestion was for 18 h at 37 °C in 1 ml of 25 mM NH_4HCO_3, pH 8, containing 100 μg of Tos-Phe-CH_2Cl-treated trypsin (Worthington), and the second for 4 h at 50 °C after the addition of 1 ml of 25 mM NH_4HCO_3, pH 8, containing 75 μg of thermolysin (Calbiochem) and 1 mM $CaCl_2$. After digestion, supernatants were collected and lyophilized. Cerenkov counting of the lyophilized peptide residues showed that more than 95% of the radioactivity was recovered from each gel piece by this method. The dried samples were solubilized in 20 μl of 1% pyridine/10% acetic acid buffer, pH 3.2. A portion (2–20 μl) was spotted in the middle of a thin cellulose plate (20 cm × 20 cm; Kodak) 4 cm from the bottom with a trace of basic Fuschin dye. Electrophoresis was carried out at 350 V in 1% pyridine/10% acetic acid buffer, pH 3.5, until the basic Fuschin dye had migrated 2.5 cm toward the cathode (45 min). The plates were air-dried and subjected to ascending chromatography in pyridine/butan-1-ol/acetic acid/water (15:10:3:12, by vol.) until the solvent front reached the top of the plate. Plates were air-dried and exposed to Kodak XAR-5 films for autoradiography.

RESULTS

Molecular characterization of recombinant stathmin and its mutant forms

Expression and purification of the wild-type and mutant forms of recombinant stathmin

We produced and purified high levels of recombinant human stathmin in a prokaryote expression system. For convenience, we will refer to the protein naturally occurring in tissues as native stathmin, that produced in bacteria as recombinant stathmin and the unmutated forms as wild-type stathmin. Two mutant forms of stathmin were also generated by *in vitro* mutagenesis (see the Materials and methods section) and similarly produced and purified: St_{63A} in which Ser-63 was replaced by alanine to suppress the major PKA phosphorylation site; St_{25E}, in which Ser-25, the major target of MAP kinases, was replaced by a glutamic acid residue in order to mimic the charge generated by the phosphate in the corresponding phosphorylated form of stathmin.

cDNAs encoding the 149-amino acid sequence of human stathmin and the two mutant forms St_{25E} and St_{63A} were cloned under the control of the T7 RNA polymerase promoter and expressed in the strain of *E. coli* BL21(DE3), containing the T7 RNA polymerase gene under the control of a *lac* UV5 promoter [42]. High-level expression of recombinant proteins of the expected molecular mass was obtained after induction with IPTG. Recombinant stathmin was purified from a soluble bacterial extract by a simple two-step procedure combining anion-exchange chromatography and gel filtration; the resulting protein migrated as a single band on one-dimensional SDS/PAGE (Figure 1a). Quantification of the pure protein by u.v. absorption at 205 nm after calibration by direct amino-acid analysis of a pure fraction shows that more than 10 mg of pure recombinant stathmin can be obtained from 1 litre of bacterial culture, similar yields being obtained with the wild-type and mutant forms.

Characterization by two-dimensional PAGE

Two-dimensional PAGE of recombinant stathmin showed the presence of a major (N) and a minor more acidic (n) form migrating at 19 kDa (Figure 1b). The apparent molecular mass and the results of amino acid analysis (see the Materials and methods section) were consistent with the hypothesis that the recombinant proteins were full length. However, the recombinant stathmin forms migrated at slightly more basic isoelectric points than the unphosphorylated forms N1 and N2 of the native protein from eukaryotic cells (Figure 1b), as confirmed also by two-dimensional PAGE co-migration experiments (not shown).

The mutant forms of recombinant stathmin also displayed two spots on two-dimensional gels (see Figures 6 and 7). As expected, the wild-type recombinant protein and St_{63A} display the same isoelectric points, whereas St_{25E} migrates at a more acidic pH as a result of the charge on the additional glutamic acid residue.

M.s. analysis of the N-terminal maturation of recombinant stathmin

As predicted [35] on the basis of its amino acid sequence, the N-terminal methionine of native stathmin in eukaryotes is cleaved and the following alanine residue is acetylated [40,47]. Following the rule established for *E. coli* [48], alanine being a short-side-chain amino acid, it was expected that the N-terminal methionine of recombinant stathmin would also be excised, but without acetylation of the resulting N-terminal alanine. To assess this hypothesis, we determined the exact mass of recombinant stathmin by m.s. (Figure 2). The mean value obtained from seven sample analyses is 17170 ± 5 Da, in perfect agreement with the average mass of 17172.4 Da calculated for recombinant stathmin starting with unmodified alanine. M.s. determinations on proteolytic peptides further confirmed this result. The observed charge difference between the native eukaryotic stathmin and the recombinant form expressed in *E. coli* is therefore probably due to the absence of acetylation of the recombinant protein.

C.d. analysis of structural features of recombinant stathmin

The production of recombinant stathmin allowed analysis of its structural features in a highly pure and concentrated form by c.d. As shown in Figure 3, the far-u.v. c.d. spectrum reveals a high content of secondary structure, mainly α-helix. This spectrum could be satisfactorily fitted to a linear combination of the four vectors of the database of Brahms and Brahms [44] between 190 and 240 nm. The best fit corresponds to 45.5% α-helix and 7.5% β-structures, with a total root mean square value of 6.28 degrees·cm^2·dmol^{-1} (for 51 data points).

In vitro phosphorylation properties of recombinant stathmin and its mutant forms

Recombinant stathmin is efficiently phosphorylated by PKA and p34cdc2 on their native target sites

We have recently shown that eukaryotic stathmin was phosphorylatable *in vitro* and *in vivo* [37] on four serine residues:

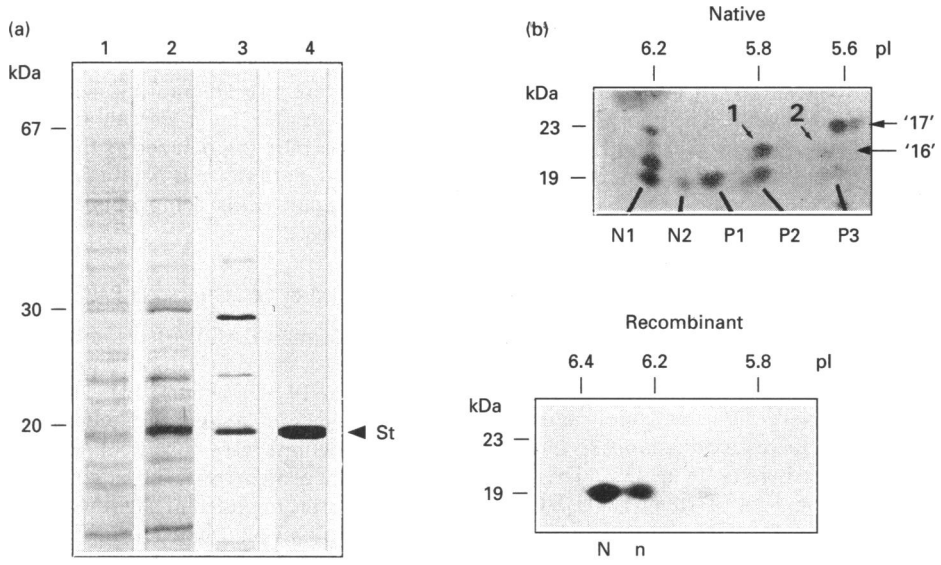

Figure 1 Expression in *E. coli* and purification of recombinant human stathmin

(**a**) Proteins from *E. coli* transformed with the pSt plasmid directing the expression of human stathmin were analysed by one-dimensional SDS/PAGE with detection by silver staining: soluble proteins (S2, see the Materials and methods section) from unstimulated (lane 1) and IPTG-stimulated (lane 2) bacteria; peak fractions eluted from the DEAE-Sepharose column (lane 3) and from the subsequent f.p.l.c. Superose 12 column (lane 4). St, stathmin. (**b**) Two-dimensional PAGE of purified recombinant stathmin compared with the pattern of unphosphorylated (N1, N2) and phosphorylated forms of stathmin in a soluble extract from human T-lymphocytes stimulated with a combination of phytohaemagglutinin (37.5 μg/ml) and phorbol 12-myristate 13-acetate (10 ng/ml) to induce phosphorylation of stathmin. For a better visualization of the minor form, n, recombinant stathmin was overloaded on the two-dimensional gel; the actual ratio of n/N was estimated at about 0.05–0.1.

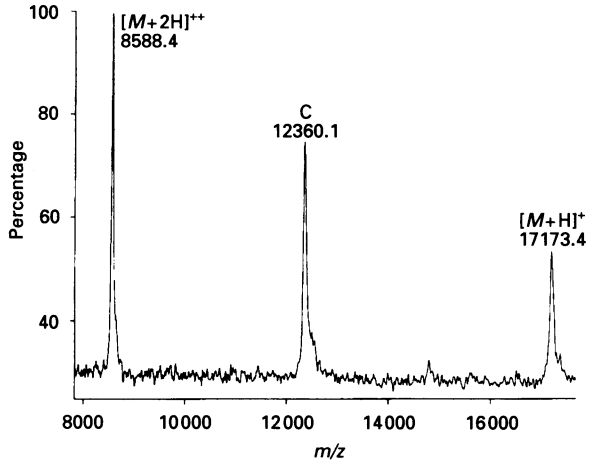

Figure 2 M.s. determination of the molecular mass of recombinant stathmin expressed and processed in *E. coli*

Pure recombinant stathmin was analysed by m.s. (see the Materials and methods section) with cytochrome *c* as an internal reference (C). The single- and double-charged pseudomolecular ions of stathmin are shown with their *m/z* values in this example of accumulated spectrum.

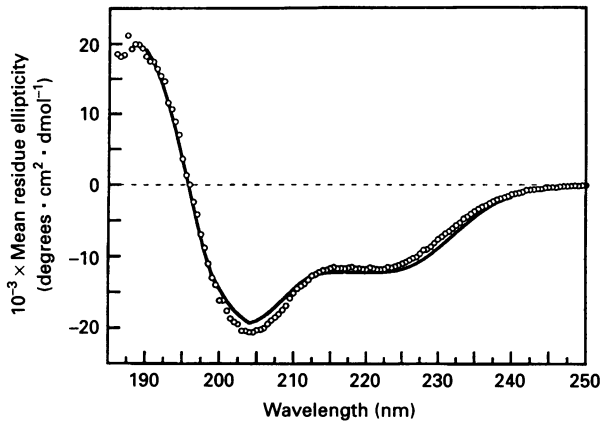

Figure 3 Far-u.v. c.d. spectrum of stathmin

The c.d. spectrum of highly purified recombinant stathmin (33.8 μM) was determined (see the Materials and methods section) and averaged from three individual scans (○). The solid line corresponds to the best-fitting theoretical spectrum obtained with a linear combination of the four components of Brahms and Brahms [44] in the following proportions: 0.455 α-helix, 0.075 β-structures, 0.01 β-turn and 0.46 unordered elements.

in vitro PKA phosphorylates Ser-63 (major site) and Ser-16 (minor site), p34cdc2 phosphorylates Ser-38 (major) and Ser-25 (minor), and MAP kinase phosphorylates Ser-25 (major) and Ser-38 (minor) [37,38] (Figures 4a and 4b). In the present work, we therefore first checked whether recombinant stathmin was phosphorylatable on the same sites by PKA and p34cdc2. After phosphorylation by PKA or p34cdc2 in the presence of [γ-^{32}P]ATP, two new 19 kDa spots, P1 and P2, were detected by two-dimensional PAGE by both silver staining and autoradiography (see Figure 5a for PKA). Phosphopeptide analysis of the radioactive phosphoforms (Figure 4c) showed the incorporation of phosphate in the same respective sites (Ser-63 and Ser-16 with PKA and Ser-38 and Ser-25 with p34cdc2) and in similar relative proportions to those in native mouse and human stathmin [37]. These results clearly indicate that recombinant stathmin has phosphorylation properties similar to those of the native molecule.

With PKA, more detailed analysis of the sites phosphorylated in each spot revealed indeed that, as expected for normal

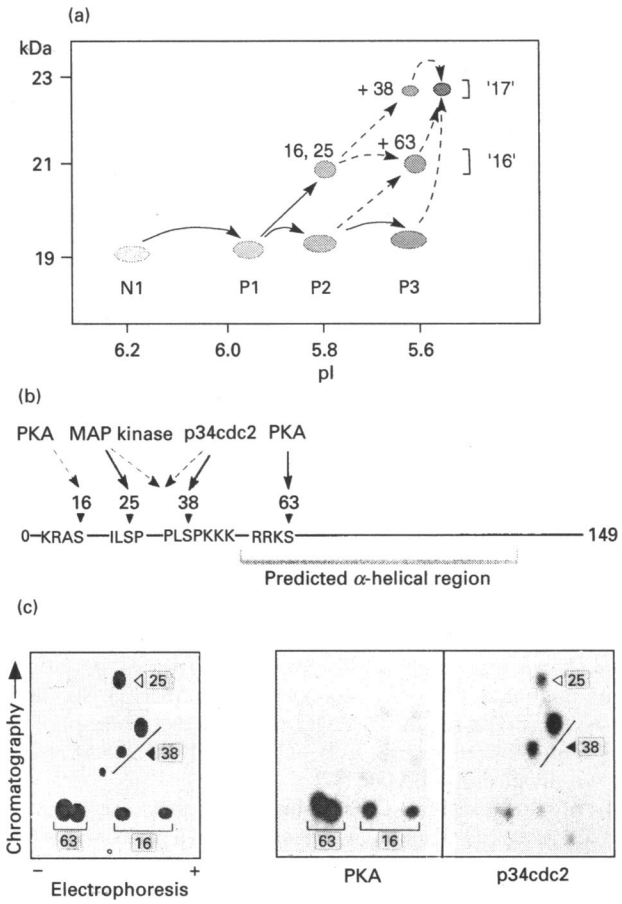

Figure 4 Phosphorylation sites of recombinant stathmin by PKA and p34cdc2

As a reference, (**a**) the two-dimensional PAGE pattern of the non-phosphorylated (N1) and phosphorylated forms of the major (α) isoform of native stathmin is presented schematically with numbers indicating the sites phosphorylated in the low-mobility forms '16' and '17', and (**b**) the sequence of stathmin is shown with the major (full arrows) and minor (broken arrows) *in vitro* phosphorylation sites for the kinases indicated [37,38]. (**c**) Pure recombinant stathmin was phosphorylated *in vitro* in the presence of [γ-^{32}P]ATP and analysed by phosphopeptide mapping as described in the Materials and methods section: a composite two dimensional phosphopeptide map pattern including the spots corresponding to each of the four sites identified [37] is presented on the left, and the actual maps obtained after phosphorylation by PKA and p34cdc2 respectively are to the right. The radioactive spots at the bottom of the p34cdc2 map are due to minor impurities in the kinase preparation with some contaminating phosphorylation activity.

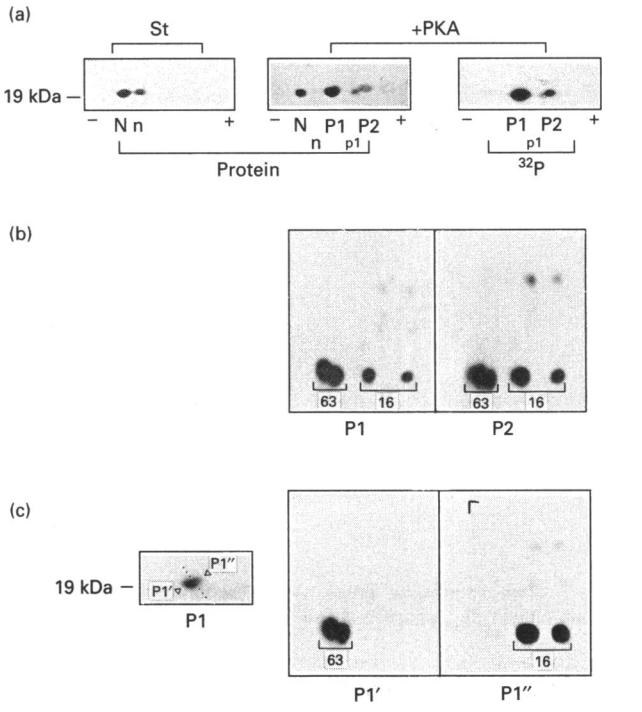

Figure 5 Two-dimensional PAGE and phosphorylation-site patterns of recombinant stathmin phosphorylated by PKA

Purified recombinant stathmin (St) was phosphorylated *in vitro* by PKA in the presence of [γ-^{32}P]ATP and analysed (**a**) by two-dimensional PAGE followed by silver-staining for protein detection and autoradiography for detection of the incorporated phosphate into the phosphoforms generated by PKA. N and n designate the non-phosphorylated forms of stathmin, and P1/P2 and p1 the phosphorylated spots generated from N and n respectively. (**b**) Two-dimensional phosphopeptide determination of the sites phosphorylated in spots P1 and P2, showing greater phosphorylation of Ser-63 than Ser-16 in P1 and an equal phosphorylation of both sites in P2 (the minor upper doublets above spots 16 are the result of incomplete proteolytic digestion). (**c**) On high-resolution gels and with low autoradiographic exposure, spot P1 could be resolved into a major spot P1′ and a closely migrating minor one P1″, corresponding to the phosphorylation of Ser-63 and Ser-16 respectively.

stathmin, P1 corresponds to a mixture of stathmin molecules phosphorylated on either Ser-16 or Ser-63, with the latter being the major form, whereas P2 corresponds to molecules phosphorylated on both sites (Figure 5b). Further examination of the two-dimensional autoradiograms at high resolution after short exposure times revealed that spot P1 is in reality composed of a major spot P1′ close to a minor spot P1″ migrating slightly more slowly in the SDS/polyacrylamide gel (Figure 5c). Phosphopeptide analysis of both spots showed that P1′ and P1″ correspond to the phosphorylation of stathmin on Ser-63 and Ser-16 respectively (Figure 5c), also confirming that Ser-63 is the major target for PKA. Furthermore, this observation suggests that phosphorylation of Ser-16 induces, in addition to the expected charge shift, a specific modification of the molecular structure of stathmin leading to its reduced mobility (see also below).

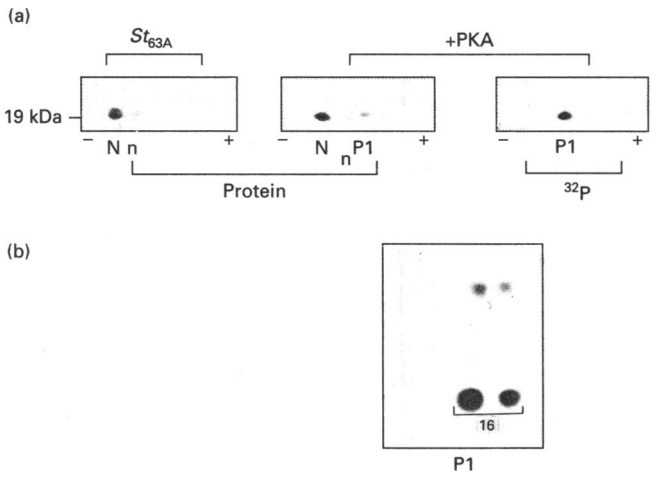

Figure 6 Two-dimensional PAGE and phosphorylation-site patterns of stathmin mutant St_{63A} phosphorylated by PKA

Purified St_{63A}, in which Ser-63 is replaced by alanine, was phosphorylated *in vitro* by PKA and analysed as in Figure 5. Two-dimensional patterns (**a**) show a much weaker phosphorylation than with the wild-type protein and the generation of only P1, phosphorylated exclusively on Ser-16 (**b**).

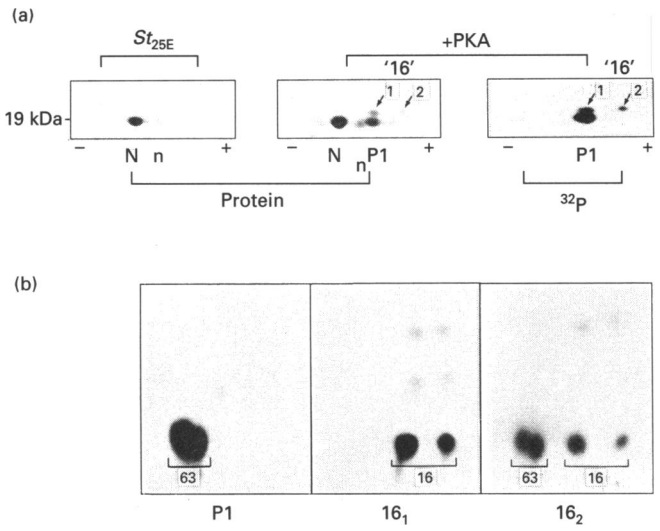

Figure 7 Two-dimensional PAGE and phosphorylation-site patterns of stathmin mutant St_{25E} phosphorylated by PKA

Purified St_{25E}, in which Ser-25 is replaced by glutamic acid, was phosphorylated *in vitro* by PKA and analysed as in Figure 5. Two-dimensional patterns (**a**) show the generation, in addition to a 19 kDa form P1, of low-mobility forms 16_1 and 16_2, phosphorylated respectively on Ser-63 (P1), Ser-16 (16_1), and equally on Ser-16 and Ser-63 (16_2) (**b**).

PKA phosphorylates St_{63A} at a single site on Ser-16

After *in vitro* phosphorylation of St_{63A} by PKA, silver staining of proteins on two-dimensional polyacrylamide gels showed the generation of a faint more acidic 19 kDa spot P1, corresponding to the single radioactive spot revealed on the autoradiogram (Figure 6). Phosphopeptide mapping revealed that this spot corresponds to the phosphorylation of St_{63A} exclusively on Ser-16. We estimate that the radioactivity incorporated into spot P1 of St_{63A} was about 10 times less than the cumulated radioactivity incorporated under the same labelling conditions into spots P1 and P2 generated by PKA phosphorylation of wild-type recombinant stathmin. These results confirm that Ser-63 is the major PKA phosphorylation site of wild-type stathmin, and that, even in the absence of this phosphorylation target, Ser-16 is a relatively poor substrate for this kinase.

St_{25E} mimics the mobility changes induced by the presence of phosphate on Ser-25

As expected, the mutated stathmin, St_{25E}, migrated with a more acidic pI on two-dimensional PAGE than wild-type recombinant stathmin. However, this acidic shift was slightly smaller than that observed after the addition of one phosphate on recombinant stathmin (shift from N to P1), indicating that, at the pH corresponding to the pI of non-phosphorylated stathmin, one phosphate induces an average charge shift that is slightly larger than the single charge shift induced by glutamate. Interestingly, phosphorylation of St_{25E} by PKA generated a single new 19 kDa spot, P1, and two other spots, 16_1 and 16_2, migrating with reduced mobility on the second-dimension SDS/polyacrylamide gel (Figure 7). Phosphopeptide mapping of the radioactive spots revealed that P1 was phosphorylated exclusively on Ser-63, whereas both spots 16_1 and 16_2 were phosphorylated on Ser-16, with Ser-63 being also phosphorylated in 16_2. Again for this mutant stathmin, Ser-63 appears to be the major target for PKA. Furthermore, the generation of low-mobility forms is similar to the generation of similar forms 16_1 and 16_2 with native stathmin, when Ser-25 is phosphorylated by p34cdc2 and Ser-16 and Ser-63 by PKA [37], although the difference in mobility is slightly less pronounced than with the native protein. The replacement of Ser-25 by glutamic acid thus mimics the phosphorylation of Ser-25 at least to the extent that it reproduces the suggested molecular interactions of phosphoserine-25 with phosphoserine-16 as they are revealed by the reduced mobility of the resulting proteins on SDS/polyacrylamide gels.

DISCUSSION

Stathmin, a ubiquitous cytosoluble 19 kDa phosphoprotein that is a substrate *in vitro* and most probably *in vivo* for at least three major kinases involved in intracellular transduction and regulatory cascades, PKA, p34cdc2 and MAP kinase [18,34,37–39,49,50], has been proposed to be a relay protein, possibly integrating multiple signals that control proliferation, differentiation and other functions of cells during development and adult life [22]. Its phosphorylation on four distinct sites is finely regulated in many different biological systems in response to numerous extracellular signals and biological situations (reviewed in [2]). Molecular studies of stathmin in the laboratory have shown that, both *in vitro* and *in vivo*, phosphorylation of combinations of the same four sites (Ser-16, Ser-25, Ser-38 and Ser-63) accounts for the diversity of its up to 14 phosphoforms (apparent molecular mass $\approx$ 19–23 kDa, pI $\approx$ 6.2–5.6) resolved by two-dimensional PAGE [37].

To obtain a greater understanding of the structure, regulation and functions of stathmin, as well as to design molecular tools to interfere with the signal-transduction cascades in which stathmin is implicated, we produced and characterized human stathmin in *E. coli*, as well as forms of the protein in which some of the phosphorylation sites were replaced by neutral or charged amino acids.

Stathmin can be expressed in bacteria at levels as high as 20% of total bacterial protein, and can be extracted for purification in a simple soluble form. This behaviour is probably related to its highly charged nature and its extreme solubility even under boiling conditions [22]. This allowed us to purify large amounts of the protein, tens of milligrams compared with tenths of milligrams obtained from brain, enough to permit structural studies for characterization of the molecule.

Characterization of the purified recombinant stathmin revealed that it had biochemical properties very similar to those of the native protein, including its behaviour on purification columns. In particular, it is a good substrate for both PKA and p34cd2, the same four sites as in the native eukaryotic protein being involved. As shown by m.s., the slight difference in isoelectric point is probably due to the known protein-processing differences between eukaryotes and prokaryotes, namely the absence of acetylation of the protein produced in bacteria. On the other hand, cleavage of the N-terminal methionine occurred in the recombinant protein, as expected [48] on the basis of the second short-chain amino acid, alanine, and as predicted [35] and verified [40,47] with the native protein. The modification leading to the minor form (n) of the recombinant protein has not yet been elucidated.

The easy isolation of large quantities of highly purified recombinant stathmin has allowed the determination of its u.v.-absorption spectrum and molar absorption coefficients, valuable tools also for its quantification for further structural studies. C.d. studies showed that stathmin is likely to contain about 45% of its sequence in an α-helical conformation. Also in agreement with the highly elongated shape of the molecule as determined by

molecular-sieve chromatography [50], this result is strongly in favour of the existence of an α-helical region, as predicted by computer analysis of the amino acid sequence of stathmin, between residues 47 and 124 [35], representing about 53% of the entire sequence. As the same region contains characteristic heptad repeats of neutral and hydrophobic residues, it also strongly supports the predicted possibility of 'coiled-coil' interaction of stathmin [35] (and stathmin-related proteins such as SCG10 [51]) with proteins presenting similar structures.

PKA phosphorylates native [37], as well as recombinant stathmin mostly on Ser-63, and less efficiently on Ser-16. This was confirmed by the fact that the replacement of Ser-63 by alanine indeed suppressed the major phosphorylation site and that this mutant form of stathmin was about ten times less efficiently phosphorylated by PKA, solely on Ser-16, than the native protein. This result indicates that the relatively poor substrate nature of this site is intrinsic, and is not due, in the wild-type protein, to competition with phosphorylation of Ser-63. Ser-16 is preceded by the sequence KRA, which is known to be less favourable for PKA than the RRK sequence preceding Ser-63. Furthermore, at least in some *in vivo* conditions, it seems that Ser-16 is better phosphorylated than Ser-63, as can be deduced for example from the pattern of phosphoforms generated in T-lymphocytes in response to their activation by CD2 [14]. It is thus likely that Ser-16 is not a significant phosphorylation site of PKA *in vivo*, but may be of some other kinase(s) yet to be identified.

Two other serines in the stathmin sequence, Ser-25 and Ser-38, have been found to be phosphorylated *in vivo* [37,40,52] and shown to be substrates *in vitro* for p34cdc2 [37] and MAP kinase(s) [38]. We have shown recently that Ser-25 is a direct substrate *in vivo* for MAP kinase in PC12 cells when their differentiation to a neuronal phenotype is stimulated by nerve growth factor [38]. Both *in vitro* and *in vivo* experiments demonstrated that the combined phosphorylation of Ser-16 and Ser-25 leads to a reduced mobility of the resulting proteins on the SDS dimension of two-dimensional gels which is further enhanced by phosphorylation of Ser-38 [37], suggesting that interactions between these sites might lead to specific conformational changes which are probably also related to the functional regulation of stathmin.

Interestingly, it appeared in the present work that stathmin phosphorylated on Ser-16 migrates with a slightly reduced mobility on SDS/polyacrylamide than the protein phosphorylated on Ser-63. The reduction in mobility is, however, much more pronounced if both Ser-16 and Ser-25 are phosphorylated. It is interesting that the replacement of Ser-25 by the charged amino acid, glutamic acid, which did not induce any substantial mobility shift by itself, nor did it interfere with the phosphorylation of stathmin by PKA (even the ratio of phosphorylation of Ser-63 and Ser-16 is unchanged), reproduced, at least to a large extent, the effect of phosphoserine-25 on the mobility shift induced in conjunction with phosphorylation of Ser-16. It will be interesting to determine with such mutants if the phosphorylation of some sites depends on the phosphorylation of others, introducing for example a 'sequentiality' [2,19] into the regulation of stathmin through phosphorylation.

The nature of the molecular processes underlying the observed decreases in electrophoretic mobility is unknown. Clearly the electric charge contributed by the phosphate group or the acidic group of glutamate is the main component, although steric factors might also have a role. The slightly lower mobility shift induced by glutamate than by phosphate is probably due to the smaller charge on average contributed by glutamate than by phosphate at the pH considered. In both cases, however, the reduced mobility may be due to different interactions with SDS or, more likely, to local conformational changes possibly also related to the proximity of several proline residues, at least for the contribution of residues 25 and 38.

Although it is not always the case, replacement of serine- or threonine-phosphorylation sites by charged amino acids can reproduce the regulatory action(s) of phosphorylation [53,54]. In the case of stathmin, the reproduction of the mobility shift suggests that the regulation of functional properties brought about by phosphorylation of Ser-25 might also be mimicked by its replacement by glutamic acid.

Altogether, characterization of recombinant stathmin and its mutant forms gives good indications of the structure of stathmin and the molecular mechanisms of its biological regulation related to the control of cell function, proliferation and differentiation. It further indicates that the wild-type recombinant protein, as well as mutants in which the various phosphorylation sites are replaced by alanine to prevent phosphorylation or by a charged amino acid to mimic it, are valuable tools for use in the elucidation of the regulatory mechanisms and function(s) of stathmin, through biochemical and structural experiments *in vitro* and functional experiments *in vivo* after expression or introduction of the corresponding proteins into cells.

We thank Dr. M. Fardeau and Dr. S. Blanquet for their constant support, Dr. F. W. Studier and Dr. P. Charnay for providing plasmids and host strains of the T7 RNA polymerase overexpression system, Dr. J. A. Girault for his advice and help with mutagenesis and phosphorylation experiments, Dr. L. Beretta for her help with phosphorylation experiments, Dr. T. Dobransky for his help with purification experiments, Dr. S. le Gouvello for the gel of native stathmin from human lymphocytes, B. M. C. Hoang for her help with m.s. measurements, and Dr. M. Dorée and Dr. J. C. Labbé for the gift of p34cdc2. This work was supported by funds from the Institut National de la Santé et de la Recherche Médicale, the Centre National de la Recherche Scientifique, the Association Française contre les Myopathies, the Association pour la Recherche contre le Cancer, the Ligue Nationale Française contre le Cancer, the Ecole Polytechnique and the Fondation Nationale de Transfusion Sanguine.

REFERENCES

1 Sobel, A. and Tashjian, A. H., Jr. (1983) J. Biol. Chem. **258**, 10312–10324
2 Sobel, A. (1991) Trends Biochem. Sci. **16**, 301–305
3 Pasmantier, R., Danoff, A., Fleischer, N. and Schubart, U. K. (1986) Endocrinology **19**, 1229–1238
4 Schubart, U. K, Xu, J., Fan, W., Cheng, G., Goldstein, H., Alpini, G., Shafritz, D. A., Amat, J. A., Farook, M., Norton, W. T., Owen, T. A., Lian, J. B. and Stein, G. S. (1992) Differentiation **51**, 21–32
5 Braverman, R., Bhattacharya, B., Feuerstein, N. and Cooper, H. L. (1986) J. Biol. Chem. **261**, 14342–14348
6 Cooper, H. L., Fuldner, R., McDuffie, E. and Braverman, R. (1991) J. Immunol. **146**, 3689–3696
7 Hanash, S. M., Strahler, J. R., Kuick, R., Chu, E. H. Y. and Nichols, D. (1988) J. Biol. Chem. **263**, 12813–12815
8 Luo, X.-N., Arcasoy, M. O., Brickner, H. E., Schechter, A. D. and Atweh, G. F. (1991) J. Biol. Chem. **31**, 21004–21010
9 Hailat, N., Strahler, J. R., Melhem, R. F., Zhu, X. X., Brodeur, G., Seeger, R. C., Reynolds, C. P. and Hanash, S. M. (1990) Oncogene **5**, 1615–1618
10 Gullberg, M., Noreus, K., Brattsand, G., Friedrich, B. and Shingler, V. (1990) J. Biol. Chem. **265**, 17499–17505
11 Peyron, J.-F., Aussel, C., Ferrua, B., Häring, H. and Fehlmann, M. (1989) Biochem. J. **258**, 505–510
12 Beretta, L., Boutterin, M. C. and Sobel, A. (1988) Endocrinology **122**, 40–51
13 Mary, D., Peyron, J. F., Auberger, P, Aussel, C. and Fehlmann, M. (1989) J. Biol. Chem. **264**, 14498–14502
14 le Gouvello, S., Chneiweiss, H., Tarantino, M., Debre, P. and Sobel, A. (1991) FEBS Lett. **287**, 80–84
15 Strahler, J. R., Hailat, N., Lamb, B. J., Rogers, K. P., Underhill, J. A., Melhem, R. F., Keim, D., Zhu, X. X., Kuick, R., Fox, D. A. and Hanash, S. M. (1992) J. Immunol. **149**, 1191–1198
16 Meyer, N., Prentice, D. A., Fox, M. T. and Hughes, J. P. (1992) Endocrinology **131**, 1977–1984
17 Doye, V., Boutterrin, M. C. and Sobel, A. (1990) J. Biol. Chem. **265**, 11650–11655

18 Chneiweiss, H., Beretta, L., Cordier, J., Boutterin, M. C., Glowinski, J. and Sobel, A. (1989) J. Neurochem. **53**, 856–863
19 Chneiweiss, H., Cordier, J. and Sobel, A. (1992) J. Neurochem. **58**, 282–289
20 Toutant, M. and Sobel, A. (1987) Dev. Biol. **124**, 370–378
21 Schubart, U. K. (1988) J. Biol. Chem. **263**, 12156–12160
22 Sobel, A., Boutterin, M. C., Beretta, L., Chneiweiss, H., Doye, V. and Peyro-Saint-Paul, H. (1989) J. Biol. Chem. **264**, 3765–3772
23 Koppel, J., Boutterin, M. C., Doye, V., Peyro-Saint-Paul, H. and Sobel, A. (1990) J. Biol. Chem. **265**, 3703–3707
24 Amat, J. A., Fields, K. L. and Schubart, U. K. (1991) Dev. Brain Res. **60**, 205–218
25 Peschanski, M., Hirsch, E., Dusart, I., Doye, V., Marty, S., Manceau, V. and Sobel, A. (1993) J. Comp. Neurol. **337**, 655–668
26 Cooper, H. L., McDuffie, E. and Braverman, R. (1989) J. Immunol. **143**, 956–963
27 Melhem, R. F., Zhu, X. X., Hailat, N., Strahler, J. R. and Hanash, S. M. (1991) J. Biol. Chem. **266**, 17747–17753
28 Doye, V., Kellermann, O., Buc-Caron, M. H. and Sobel, A. (1992) Differentiation **50**, 89–96
29 Sobel, A., Peyro-Saint-Paul, H., Koppel, J. and Doye, V. (1989) EMBO Workshop on Cellular and Molecular Biology of Muscle Development, Cambridge, UK, September 24–29, 1989 (Abstract)
30 Melhem, R. F., Strahler, J. R., Hailat, N., Zhu, X. X., Hanash, S. M. (1991) Biochem. Biophys. Res. Commun. **179**, 1649–1655
31 Maucuer, A., Doye, V. and Sobel, A. (1990) FEBS Lett. **264**, 275–278
32 Maucuer, A., Moreau, J., Mechali, M. and Sobel, A. (1993) J. Biol. Chem. **268**, 16420–16429
33 Schubart, U. K., Das Banerjee, M. and Eng, J. (1989) DNA **8**, 389–398
34 Beretta, L., Houdouin, F. and Sobel, A. (1989) J. Biol. Chem. **264**, 9932–9938
35 Doye, V., Soubrier, F., Bauw, G., Boutterin, M. C., Beretta, L., Koppel, J., Vandekerckhove, J. and Sobel, A. (1989) J. Biol. Chem. **264**, 12134–12137
36 Doye, V., le Gouvello, S., Dobransky, T., Chneiweiss, H., Beretta, L. and Sobel, A. (1992) Biochem. J. **287**, 549–554
37 Beretta, L., Dobransky, T. and Sobel, A. (1993) J. Biol. Chem. **268**, 20076–20084
38 Leighton, I., Curmi, P., Campbell, D. G., Cohen, P. and Sobel, A. (1993) Mol. Cell. Biochem. **127/128**, 151–156
39 Marklund, U., Brattsand, G., Schingler, V. and Gullberg, M. (1993) J. Biol. Chem. **268**, 15039–15047
40 Labdon, J. E., Nieves, E. and Schubart, U. K. (1992) J. Biol. Chem. **267**, 3506–3513
41 Sanger, F., Nicklens, S. and Coulson, A. R. (1977) Proc. Natl. Acad. Sci. U.S.A. **74**, 5463–5467
42 Studier, F. W., Rosenberg, A H., Dunn, J. J. and Dubendorff, J. W. (1990) Methods Enzymol. **185**, 60–89
43 Yang, J. T., Wu, C. S. C. and Martinez, H. M. (1986) Methods Enzymol. **130**, 208–269
44 Brahms, S. and Brahms, J. (1980) J. Mol. Biol. **72**, 149–178
45 Laemmli, U. K. (1970) Nature (London) **227**, 680–685
46 Garrels, J. I. and Schubert, D. (1979) J. Biol. Chem. **254**, 7978–7985
47 Hanash, S. M., Strahler, J. R., Neel, J. V., Hailat, N., Melhem, R. F., Keim, D., Zhu, X. X., Wagner, D., Gage, D. A. and Watson, J. T. (1991) Biochemistry **88**, 5709–5713
48 Hirel, P. H., Schmitter, J. M., Dessen, P., Fayat, G. and Blanquet, S. (1989) Proc. Natl. Acad. Sci. U.S.A. **86**, 8247–8251
49 Feuerstein, N., Nishikawa, M. and Cooper, H. L. (1985) Cancer Res. **45**, 3243–3251
50 Schubart, U. K., Alago, W., Jr. and Danoff, A. (1987) J. Biol. Chem. **262**, 11871–11877
51 Stein, R., Mori, N., Matthews, K., Lo, L. C. and Anderson, D. J. (1988) Neuron **1**, 463–476
52 Wang, Y. K., Liao, P.-C., Allison, J., Gage, D. A., Andrews, P. C., Lubman, D. M., Hanash, S. M. and Strahler, J. R. (1993) J. Biol. Chem. **268**, 14269–14277
53 Hurley, J. H., Dean, A M., Sohl, J. L. Koshland, D. E. and Stroud, R. M. (1990) Science **249**, 1012–1016
54 Wang, Y. H., Duff, S. M. G., Lepiniec, L., Crétin, C., Sarath, G., Condon, S. A., Vidal, J., Gadal, P. and Chollet, R. (1992) J. Biol. Chem. **24**, 16759–16762

Received 11 October 1993/18 November 1993; accepted 3 December 1993